European Society of Computational Methods in Sciences and Engineering (ESCMSE)

Journal of Numerical Analysis, Industrial and Applied Mathematics (JNAIAM)
vol. 2, no. 3-4, 2007, pp. 115-128
ISSN 1790–8140

Modeling of Binary Collision between Multisize Viscoelastic Spheres[†]

M.H. Bordbar[‡], T. Hyppänen

Department of Energy and Environmental Technology,
Faculty of Technology,
Lappeenranta University of Technology,
P.O. Box 20, FIN-53851 Lappeenranta, Finland.

Received 15 November 2005; Revised 22 January 2007, Accepted 25 January 2007

Abstract: An accurate new contact force model is proposed for describing the grain collision process. The linear and nonlinear contact force models and normal coefficient of restitution in different impact velocities has been studied. A new contact force model for describing the normal collision between two viscoelastic spherical particles has been suggested and the ability of this new model in predicting the correct behavior of normal contact has been confirmed. The constitutive equations of this model have been solved numerically and the result shows a better conformity with experimental result reported by Bridge et al.[1] than the previous models, such as the model presented by Brilliantov et al.[2]. By using the suitable finite elements model, the stress and deformation of particles during the collision has been obtained and the result of the finite element model shows a good conformity with our new suggested contact force model in the case of elastic and viscoelastic contact. The behavior of normal coefficient of restitution in multisize spherical particles in different impact velocities and the effect of the size on it has been experimentally studied. In addition to our more suitable contact force model, we achieved some nice conclusions from our experimental data about the loss of energy during the multisize collision and effect of size difference on this loss.

Keywords: Collision, Contact-Force Model, Granular Material, Viscoelastic Particle.

Mathematics Subject Classification: 93A30

PACS: 45.50.Tn , 45.70.Vn, 07.05.Tp

1. Introduction

A granular material is a conglomeration of discrete solid, macroscopic particles characterized by a loss of energy whenever the particles interact (the most common example would be friction when grains collide). Granular materials are commercially important in applications as diverse as pharmaceutical industry, agriculture and energy production. Research on granular materials is thus directly applicable and goes back to at least Coulomb, whose law of friction was originally stated for granular materials. Collisions between particles which have a key role in transferring energy and momentum in granular systems are not well understood. Therefore, an excellent understanding of energy loss, and the amount of energy dissipation when two particles collide into each other, is one of the eminent targets of this article. In granular flow studies, the linear viscoelastic contact model considering Mohr friction law is applied most widely [3-5]. In this linear model, the normal and tangential contact forces are a linear function of the displacement and relative velocity, and the Mohr friction law controls the maximum tangential force. This linear contact model simplifies the computational procedure. Many granular flow behaviors have been studied using this simple contact force model. In fact, for most granular material,

[†] Published electronically October 27, 2007
[‡] Corresponding author. E-mail: bordbar@lut.fi

the contact force has a nonlinear relationship with relative displacement and velocity, which has been proved by experimental data and analytical solutions [6, 7].
More than one century ago, the famous Hertzain law for a non-linear, normal contact model of elastic sphere was established [8]. The original non-linear, tangential contact model was studied by Mindlin [9]. Both of them constructed the basic Hertzain-Mindlin contact theory for elastic granular materials. This theory has been applied widely. Walton et al. [10] adopted a simple plastic model to handle collision dissipation. This model was applied in several other subsequent studies [11]. Based on the Hertzain-Mindlin theory, but considering also the plastic behavior, a finite element method was used to investigate the details of a sphere colliding with a plane [12-14].
Gugan et al. [15] reported that in viscoelastic collision between two spheres, they lost about 40% of their kinetic energy over the range of their speeds studied. They also did some research about the area and duration of contact and their result was consistent with Hertz theory.
Experimental studies have been widely used for analyzing the collision phenomena. Bridges et al. [1] carried out some experiments to measure the coefficient of restitution for collision between the ice particles. They made some different ambient conditions for their experiments and set the temperature of system between 150 and 175 K. They found out how impact velocity and temperature influence normal coefficient of restitution. Their experimental result has been widely used as a trustable reference value for testing the numerical model in this field.
The aim of this article is to find sound understanding of binary collision process between two spherical particles with different diameters. Therefore, according to the history of this topic, the experiments, numerical contact force models and Finite Element Methods has been employed as the three famous approaches for achieving this target. In section 2, the experimental device and the result of experiments in the field of monosize and multisize collision between spherical particles will be explained. In section 3, a new contact force model will be presented and ability of this new model for investigating the behavior of particles during the collision will be shown. The finite elements method will be the last approach that we have employed for studying collision phenomena and it will be explained in section 4 of this article. By using finite elements method we will explain the stress behavior of two particles during the collision. By comparing the results of these three aforementioned approaches, we will reach to very useful achievement in explaining binary collision process between viscoelastic balls.

2. Experiment

One aim of this study is to further investigate collisions between inelastic spherical particles. To this end, the classical collision experiment known as Newton's Cradle was used, as shown in Figure 1. As illustrated in Figure 1, two spherical particles with certain mass and size were arranged by suspending each particle from a frame using two very thin threads. In order to ensure the elimination of the rotation of the balls their centers of mass were aligned very carefully. For the monosize collision test, two balls were chosen of the same material and size, but for the multisize collision test, the size and material of the two particles can be different. By releasing the first ball from an elevation an impact was generated which was captured using a digital camcorder DSR-PDX 10 P. By using this kind of camcorder with accuracy of 425 frames per second, we were able to find the position of center of mass of particles in each time during the collision. Reflective tapes were used to mark the center of each ball. Note that it is important to have very bright, focused light sources closely aligned with the camera axis. Using the acquired video images, the dropping height and the corresponding inclination angle with respect to the equilibrium position of the first ball, α , and the maximum post impact height attained by the other ball as well as its corresponding inclination angle, β , were determined. To generate collisions at different impact velocities, the experiments were repeated using different elevations for the first ball.

2-1. Kinematics Analysis of Collision between a Moving Spherical Particle and an Initially Stationary Spherical Particle (Newton Cradle Device)

In order to analyze the binary collision by using Newton cradle device, the governing equation of kinematics of this system should be described. In Figure 1, the positions of the balls before, at and after a collision are shown. The coefficient of restitution is:

$$e = -\frac{\text{relative velocity of particles after collision}}{\text{relative velocity of particles before collision}} \tag{1}$$

By applying an energy conservation law for the first particle in the Newton cradle device, as shown in Figure 1, we can derive the following expression for velocity of the first ball before the collision:

$$u = 2\sqrt{gl}\,\sin(\alpha/2)\,. \tag{2}$$

Where l is the length of the threads.

In the same way we can derive the following equation for velocity of the second particle after the collision (v_2) in our experiment device:

$$v_2 = 2\sqrt{gl}\,\sin(\beta/2) \tag{3}$$

Since there are no external forces on the system, the linear momentum of the system is conserved:

$$m_1 u = m_1 v_1 + m_2 v_2 \tag{4}$$

Therefore the velocity of the first particle after the collision (v_1) is:

$$v_1 = \frac{m_1 u - m_2 v_2}{m_1} \tag{5}$$

Now, we can rewrite eq.1 for finding an equation for the coefficient of restitution in a multisize binary collision:

$$e = \left(1 + \frac{m_2}{m_1}\right)\frac{\sin(\beta/2)}{\sin(\alpha/2)} - 1 \tag{6}$$

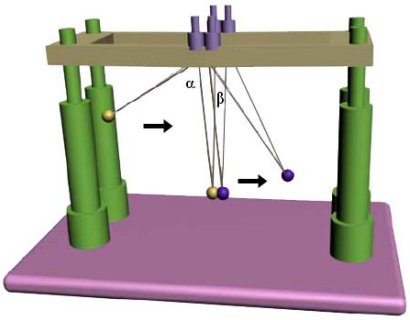

Figure 1: Schematic of apparatus used for the Newton's Cradle experiments. The balls used were spherical glass particles suspended from very thin threads.

2-2. Experimental Result

As we mentioned previously, our goal is to find the behavior of coefficient of restitution in different impact velocity for monosize and multisize collision. In this order, some glass spherical particles with properties mentioned in Table 1 have been used in different diameters; 10mm, 15.9mm, 22.2mm.We made several multisize and monosize collision with different set of particles.

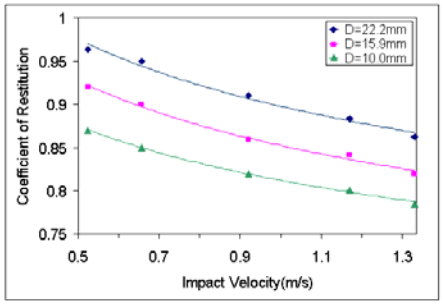

Figure 2: The variation of coefficient of restitution with impact velocity in mono-sized collisions between glass balls. In a constant impact velocity, the coefficient of restitution increases with increasing of size.

Figure2 illustrates some of our experimental result for coefficient of restitution versus impact velocities for monosize cases with different size particles. It is clear that when the size increases, the coefficient of restitution will decrease. Assuming constant impact velocity, this can be explained by the ratio of the area of contact to particle surface, which is larger for small particles than for large particles.

In our experiments, we also observed that when the two multisize particles had moved toward the monosize state, that is they had been closer in size, the coefficient of restitution increased. In fact, when the difference between radiuses of curvatures of the two particles increases, the coefficient of restitution will decrease and the amount of energy that is lost during the collision will increase. This subject has been illustrated in the Figure 3, which was made from the experimental results. This subject highlighted the role of radius of curvature in collision process. In contact region, much closer geometry will cause the smaller loss of energy and momentum.

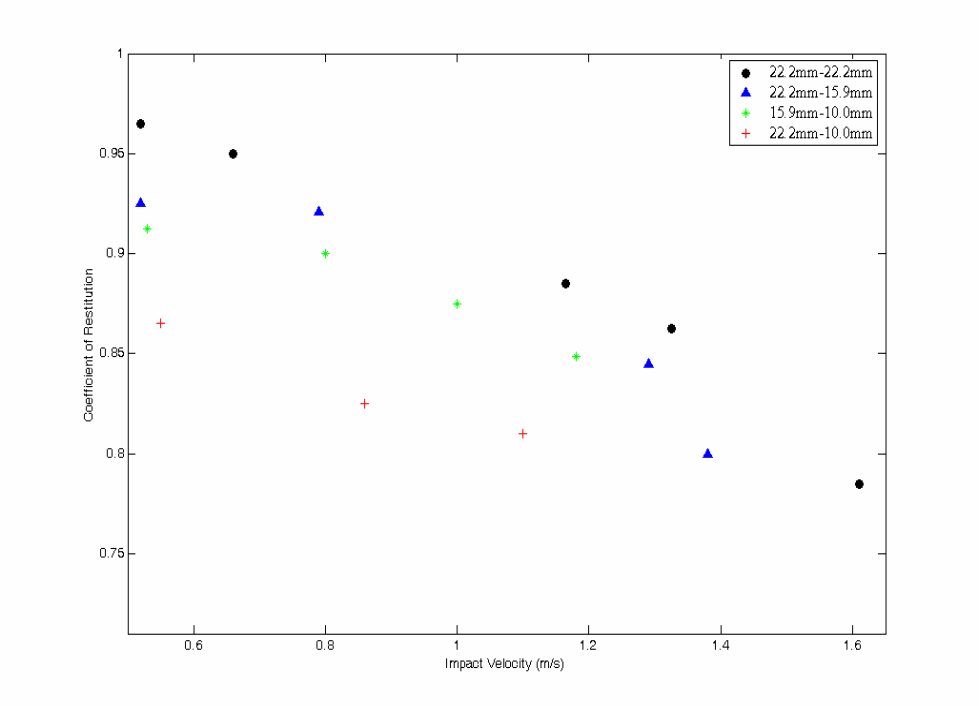

Figure 3: The variation of coefficient of restitution with impact velocity in some multisize collisions between glass balls. It seems that during one constant impact velocity, if the difference of radius of curvature between the two contact surfaces is smaller, the coefficient of restitution will be increased. In fact, we have more loss of energy in the multisize cases relative to the mono-sized cases.

3. Force Contact Model for Binary Collision

In one of most usual fields in modeling collisions, the contact action between two particles can be described with an elastic spring, viscous dashpot and friction slider. If we only consider the normal force, generally, the mechanical model is shown as Figure 4. In fact, the behavior of the materials is modeling with one simple Kelvin model. In this figure, K_e and C_e are the effective stiffness and viscosity respectively, m_1 and m_2 are the masses of the two colliding spheres.

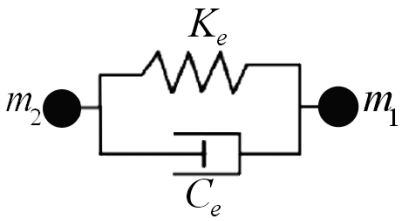

FIG.4: Particle contact model for normal force.

In this contact model, the elastic force and viscous force can be written as

$$F_e = K_e \xi^{\gamma} \text{ and } F_V = C_e \xi^n \dot{\xi} \tag{7}$$

Where ξ represents the amount of overlapping distance between the two particles, $\dot{\xi}$ is the rate of overlapping distance versus time. Based on the Newton's Second Law, the particle momentum equation is

$$m\ddot{\zeta} + C_e\zeta^n\dot{\zeta} + K_e\zeta^\gamma = 0 \tag{8}$$

Where m is the sphere mass, n and γ are the index for linear and non-linear contact models.

3-1. Linear Model

In the simple linear model, the elastic force and viscous force are the linear function of displacement and relative velocity respectively. We have $F_e = K_e\xi$ and $F_V = C_e\dot{\xi}$ when $n = 0$ and $\gamma = 1$ .Therefore, the momentum equation (Eq. 8) can be written as

$$m\ddot{\zeta} + C_e\dot{\zeta} + K_e\zeta = 0 \tag{9}$$

In the current granular flow simulations, this linear model is applied widely to study the basic physical process of complex granular systems [4, 5].

3-2. Non-Linear Model

When two spheres collide, in fact, the contact area increases with the increase of contact force. In this case, a non-linear model can describe the interaction process of the two spheres more accurately. In the non- linear model, the elastic normal force was established by Hertz [8]. In his theory there is no damping and the elastic index in Eq. 8 is $\gamma = 3/2$. This model has been proven with physical experimentations and numerical solutions [6, 17, and 18].

In the previous research for calculating viscous force, several different values for n were determined based on experimental data and analytical solution. Experiments by Falcon et al. [17] showed that it was better to set $n = 1/4$. Some analytical comparisons between a linear model and non-linear model with $n = 1/4$ have been carried out [6, 18]. It was shown that the stress, displacement and relative velocity of the two colliding spheres were simulated more reasonably with the non-linear model. In earlier studies $n = 3/2$ was also used to study the contact process [7] and determined that $n = 4/5$ and $\gamma = 8/5$ fit to their experimental results. Brilliantov et al. [2] used the nonlinear model for modeling the collision and used the following equations (10, 11) With the initial conditions $\dot{\xi}(0) = g^n$, $\xi(0) = 0$ (where g^n represents relative velocity of particles) for their model [2].

$$\ddot{\xi} + \frac{2E\sqrt{R_{eff}}}{3m_{eff}(1-\nu^2)}(\xi^{3/2} + \frac{3}{2}A\sqrt{\xi}\dot{\xi}) = 0 \tag{10}$$

In the case of $A\dot{\xi} << \xi$:

$$\ddot{\xi} + \frac{2E\sqrt{R_{eff}}}{3m_{eff}(1-\nu^2)}(\xi + A\dot{\xi})^{3/2} = 0 \tag{11}$$

Where E is Young modulus and ν is the Poisson ratio for the material of which the particles are made. The coefficient *A* was considered a fit parameter and their model's result for modeling binary collision between ice particles are shown in Figure 6.

3-3. Simplified Model for Collision of Multisize Viscoelastic Spheres

In the following section, a viscoelastic model will be presented characterized by a time dependent relation between stress and strain. Models for glass balls may be constructed by suitable combinations of springs and dashpots; where the dashpots introduce a viscous type resistance associated with internal friction in solids. Note that neither the Maxwell nor Kelvin model represents the behavior of most viscoelastic materials including the glass balls used in Newton's cradle device, illustrated in Figure 1. For example, the Maxwell model [19] predicts that the stress asymptotically approaches zero when the strain is kept constant. On the other hand, the Kelvin model does not describe a permanent strain after unloading. In this study, a second spring is placed in series with the Kelvin model used by Brilliantov et al. [2], to develop a model of linear viscoelastic material equivalent to a Maxwell model with a spring in series. The schematic of the three-parameter model used in this study is shown in Figure 5.

As we stated earlier in the section of nonlinear model, a contact force model such as $F = K\xi^{\gamma} + C\xi^{n}\, d\xi/dt$ is often adopted to capture the key features of granular inelastic interactions when the impact velocity is much less than the speed of sound in the grain material [20]. Here, $\xi = (r_1 + r_2) - |\vec{r}_1 - \vec{r}_2|$ represents the overlapping of a pair of spherical particles with radiuses $\vec{r}_1$ and $\vec{r}_2$ at positions $\vec{r}_1$ and $\vec{r}_2$, K and C are the coefficients characterizing the elastic and viscoelastic behavior of the grains, respectively.

According to calculations for elastic and viscoelastic force between particles has been done by Brilliantov and Poschel [21], The total force acting between particles during the collision can be calculated by following equations.

$$F = K\left(\xi^{3/2} + \frac{3}{2}A\sqrt{\xi}\dot{\xi}\right) \tag{12}$$

where

$$K = \frac{2E}{3(1-\upsilon^2)}\sqrt{R_{eff}} \tag{13}$$

Therefore indeed, by comparing this equation with eq.8, we will have $\gamma = 3/2, n = 1/2$ and $C = 3/2AK$ when A represents a parameter for fitting behavior.

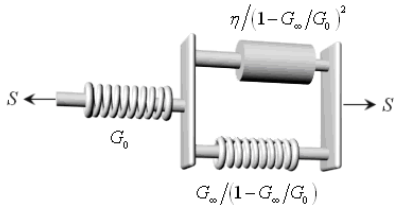

Figure 5: Model consists of auxiliary spring in series with Kelvin model.

The $\xi^{1/4}$ dependence of contact force on viscous dissipation observed in experiments [17] appears to be at odds with the $\xi^{1/2}$ scaling predicted by the Morgado and Oppenheim model [22]. Moreover, Hunt and Crossley [23] have suggested that by equating the energy loss derived from the momentum impulse approach, and that derived from hysteretic damping, an expression for the coefficient C in Eq. (13) may be found as $C = 3K(1-e^2)/4V_{imp}$, where e is the coefficient of restitution which is a measurable parameter relating the pre and post relative velocities in a collision, and V_{imp} is the relative velocity of the grains before impact. It is surprising that in [23] the $\xi^{3/2}$ dependence of contact force on the viscous dissipation was assumed.

Schwager and Pöschel [24] have suggested that for colliding viscoelastic grains with radii R_1 and R_2 and masses m_1 and m_2, the coefficient C depends on the Young modulus, the viscous constants and the Poisson ratio of the material:

$$C = C_n \frac{E}{m_{eff}\left(1-\nu^2\right)}\left(R_{eff}\right)^{1/2}, \tag{14}$$

here C_n is the normal damping coefficient,

$$m_{eff} = m_1 m_2/(m_1 + m_2) \tag{15}$$

and

$$R_{eff} = R_1 R_2/(R_1 + R_2) \tag{16}$$

The form of expression (14) was later revised by Morgado and Oppenheim [22]. They suggested that C has the same form as K, namely Eq. (13), with E and ν replaced by η_1 and η_2, respectively. Here η_1 and η_2 are the corresponding viscoelastic coefficients. These coefficients, however, are not easy to find in the literature [24].

We tried to modify this equation for two particles that are different in material and define effective Young modulus as the following equation:

$$\frac{1}{E_{eff}} = \frac{(1-\nu_1^2)}{E_1} + \frac{(1-\nu_2^2)}{E_2} \tag{17}$$

Brilliantov et al. [2] consider a Kelvin model the same as shown in Figure 4 for modeling a monosized collision. They considered the Kelvin model for modeling the viscoelastic behavior of spherical particles but we know that the real materials are not exactly Kelvin material. Therefore, as you see in Figure 5 we have added one spring in series with Kelvin model for modeling viscoelastic behavior of the particles. Now we modify the previous equation for governing the multisize and multi-material state. Therefore, the following equation will be explaining the force between the two particles in this state:

$$F = \frac{4E_{eff}\sqrt{R_{eff}}}{3m_{eff}}\xi^{\frac{3}{2}} + 2A\frac{E_{eff}R_{eff}^{(1-n)}}{m_{eff}}\xi^n\dot{\xi} \tag{18}$$

This force is acting on both particles in the opposite directions. Therefore, we can calculate acceleration of each particle from the following equation:

$$\left(\frac{d^2\xi}{dt^2}\right)_{particle\ i} = F \times \frac{m_{eff}}{m_i} \tag{19}$$

We know that if we put $n = 1/2$ in these equations (18, 19) this model becomes the same as the model that was used by Brilliantov et al. [2] and we review that in equations (10, 11). The initial conditions for Eq. (18) are $\xi(0) = 0$ and $\dot{\xi}(0) = 2\sqrt{gl}\sin\alpha/2$. The coefficient of n and A should be changed to obtain the best conformity with the experimental result.

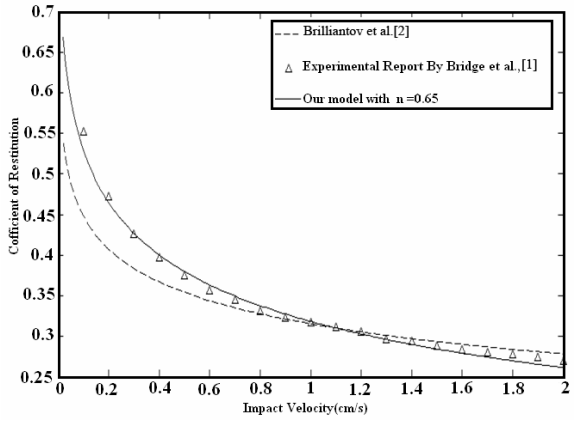

Figure 6: Coefficient of restitution in several different impact velocities measured in (cm/s) for a spherical ice particle in the diameter of $1cm$ for our model in comparison with the experimental result reported by Bridge et al [1] and the model of Brilliantov et al. [2].

To find the best model for viscoelastic collision between ice particles in low temperature with following properties [25]: Young modulus $E = 10GPa$, Poisson ratio $\nu = 0.3$, and particle size $D = 2cm$, with density $\rho = 1000kg/m^3$ we try to fix A and n with following method.

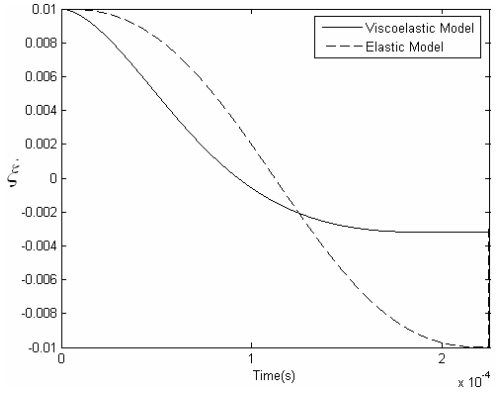

Figure 7: $\dot{\xi}$ in collision between two ice particles with diameter of 2 cm, and material properties of which is mentioned in the text, for Elastic state and Viscoelastic collision (our model n=0.65). One particle is stationary at the start of the collision and the other one has the velocity of 1cm/s.

From the previous research, which was reviewed in section 3-2, the acceptable range for n is 0.4 to 1.5. Therefore, we tried to solve the model with several values for n. For each n, we used constant A in the equation (18) as a fitting parameter for finding the best curve for which in our model obtains the greatest conformity with the experimental result reported by Bridge et al. [1]. In this step we calculated the best value for A in a least squares sense for each n and after calculating the best value for A, we calculated the least square sense for each n according the calculated value for A, then we compared values of the lease square sense together for finding the best value for n.

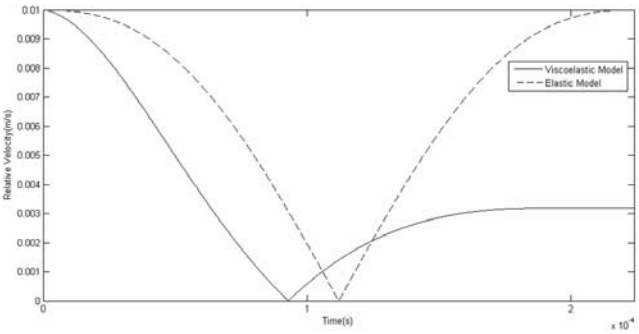

Figure 8: Velocity of first particle measured in (m/s) in the collision between two ice particles with a diameter of 2 cm, and material properties of which is mentioned in the text, for Elastic state and Viscoelastic collision (our model n=0.65). Another particle is stationary at the start of collision.

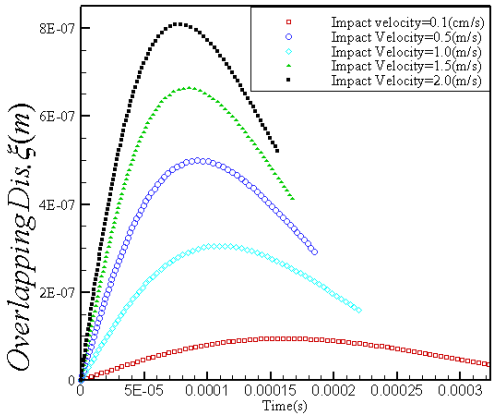

Figure 9: Effect of impact velocity on the overlapping distance ξ measured in (m) for the collision between two ice particles with diameter of 2 cm, and properties of which is mentioned in the text, for Elastic state and Viscoelastic collision (our model n=0.65). One particle is stationary at the start of the collision and the other one has several different velocities.

At the end of this process, we found that n = 0.65 had the greatest conformity with the experimental result. In Figure 6 this conformity was shown. By solving this model numerically the coefficient of restitution, which is defined as $e_n = -\dot{\xi}(t_c)/\dot{\xi}(0)$ will be calculated. Figure 7 and Figure 8 show the result of our model for the behavior of $\dot{\xi}$ and velocity of first particle in elastic collision and viscoelastic collision when the impact velocity equals to 1 cm/s. In the monosized case, when the impact velocity increases then the $\xi, \dot{\xi}, \ddot{\xi}$ will also increase. For example, Figure 9 illustrates the effect of impact velocity on the overlapping distance (ξ) for spherical ice particles with 2cm diameter.

By increasing the impact velocities the amount of overlapping distance during the collision will be increased. The amount of deformation at the end of collision that remains in the particles as the permanent deformation will also increase with increasing the impact velocity.
For glass balls with the properties mentioned in Table 1, by using the result of monosize experiment for particles with diameter of 15.9 mm as the reference values and by using the same method we found $n=1$ as the best power in our simplified model. By using this model, Zamankhan and Bordbar derived power law dependence for normal coefficient of restitution on the impact velocity [12].

4. Finite Element Method Approach in Modeling Multisize Collision

To solve stress distribution in the contact region of two multisize spherical particles and find more information about the loss of energy in a binary collision for viscoelastic materials, Finite Elements Method has been employed. Figure 10 (a) shows two spheres with a frictionless rigid planar surfaces, colliding with each other. The initial conditions are as follow; the smaller particle is stationary at first and the second one moves at $t=0$ with a certain velocity of $V_{imp.}$.

In our nonlinear dynamic finite elements model, the size and the material properties of the spheres are chosen as following; radius of the large sphere is 22.2mm and radius of the smaller one is 15.9mm. Young's modulus, Poisson's ratio and density are the same as listed in Table 1.

Properties	Symbol	Value
Elastic modulus	E	6.3×10^{10} Pa
Density	ρ_p	2390 kg/m^3
Poisson's ratio	ν	0.244
Instantaneous shear modulus	G_0	2.53×10^{10} kg/ms
Long time shear modulus	G_∞	0
The relaxation time	τ	1.676×10^{-4} sec
The coefficient characterizing the viscous behavior of grains	K_n	100

Table 1: Material properties of glass particles that have been used in the simulation of binary collision.

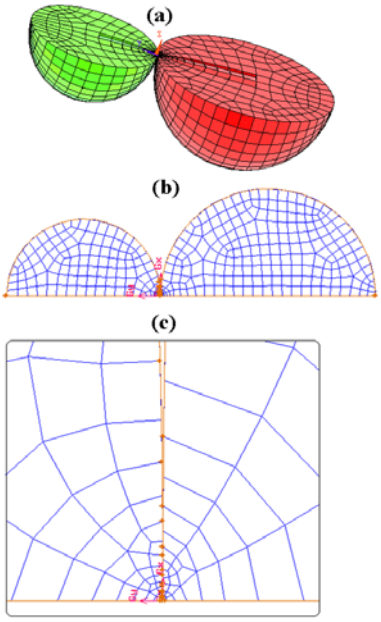

Figure 10 : (a) A schematic of a sample that we modeled with FEA. According to asymmetric property, we simplify the 3D to 2D mesh model and just analyze one half circle of two spheres that contact to each other in one single point in the beginning of collision. (b) An illustration of the meshing used in

our 2D Finite Elements model. We used a square element with high refinement around the contact area.
(c) Magnified view of the meshes near the contact region.

Since there is no particle rotation in the collision that we studied, asymmetric FE models are employed to carry out the analyses. Figure 10 (b) shows one of the meshes employed in our FEA. In this FE model, the half sphere is discretized into 2354 square elements, Figure 10 (b), with a total of 6122 nodes, and with high levels of mesh refinement around the contact area Figure 10 (c).For low velocity impacts, the deformation of the sphere during a collision is concentrated in a small region around the contact area (see later results, such as the contours of stress in contact direction presented in Figure 14). In order to accurately represent the overall response, we refine the FE mesh in the small region close to the contact point (Figure 10 (c)).
For the FE model shown in Figure 10, the size of the contact elements around the contact area is about $1.4\times10^{-5}m$, which is much less than the radius of the contact area. For example, the maximum radius of contact area is about $3.1\times10^{-4}m$ for the elastic collision with an incoming velocity of $V_{imp.}=0.5m/s$. Therefore, it can be concluded that the discretization of the sphere is fine enough especially close to contact region to describe the collision behavior accurately.

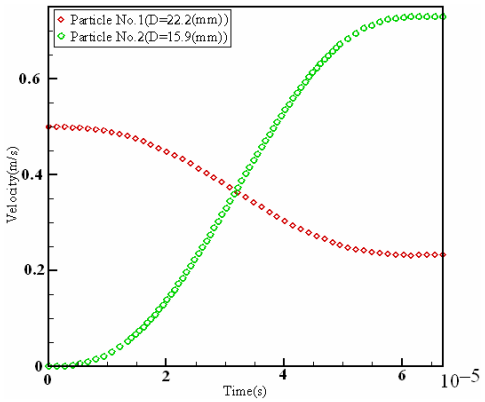

Figure 11: Velocity behavior for two sphere particles during the elastic collision. For this case, $V_{imp}=0.5(m/s), D_1=22.2mm, D_2=15.9mm$ and collision time is 6.423×10^{-5} sec .

Figure 11 shows how velocities of particles change during the elastic collision in the case of $V_{imp}=0.5(m/s), D_1=22.2mm, D_2=15.9mm$ .We calculated the coefficient of restitution from this figure as approximately 0.994, which is very close to one. This nearness confirms that our FM model has good validity for predicting the behavior of an elastic collision and therefore it is acceptable to use this mesh for simulating a viscoelastic collision.

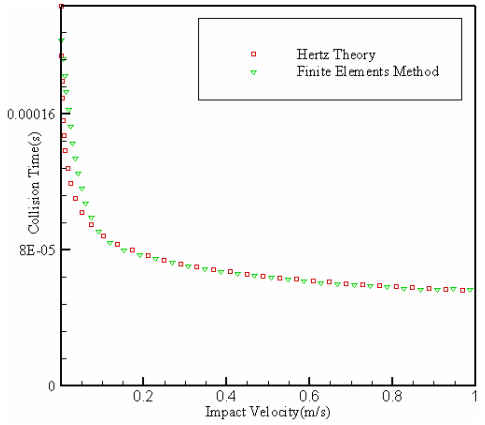

Figure 12: Collision time versus velocity of impact for two glass spheres. Their properties are listed in Table 1. The sizes of the particles are $D_1=22.2mm, D_2=15.9mm$.

One of the important parameters that have been under focus by researchers is the time of the collision. Figure 12 represents the collision time from the result of FEM for two spheres $D_1 = 22.2mm, D_2 = 15.9mm$ in comparison with the results with Hertz theory, which is validated for elastic collision and can be found in many reference books [26]. It is clear that collision time decreases with increasing velocity of impact, and the average of collision time for this range of size is about $8\times10^{-5}(s)$ .Figure 12 shows that the result of FEM for elastic collision is in good conformity with Hertz theory for predicting collision time. In Figure 13, we presented the result of the stress in direction of contact σ_{yy} during the collision for several different impact velocities. In all velocities, we saw that for elastic collision there are two steps in collision; first is the compression part, and then the second step is the separation part. In the compression step stress (pressure) increases to a maximum value in maximum deformation and after that decreases to zero, which occurs when the two particles completely separate from each other. In addition, we can see from Figure13 that when impact velocity increases the absolute value of maximum stress (pressure) will increase and time of the collision will decrease. Therefore, for the higher velocities, a larger force is acting on the particles in a shorter period, therefore, energy losses will be greater than in the cases with lower impact velocities.

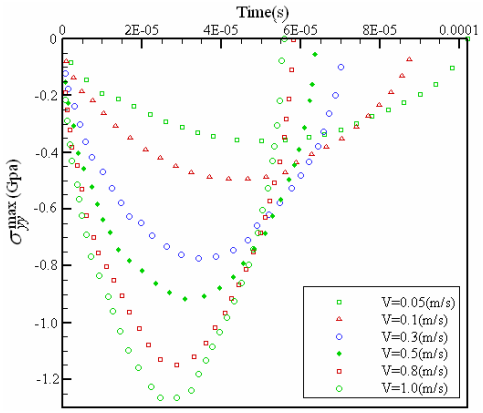

Figure 13: Stress behaviors in a multisize collision between two glass particles, their properties are listed in Table1. The sizes of the particles are $D_1 = 22.2mm, D_2 = 15.9mm$. The range of elastic stress in this case for range of impact velocities lower than 1 m/s is $-1.3Gpa$.

The distribution of stress in the contact area is one of the most important things that are interesting for us to know more. When we can make estimation about the area that is under the affect of the collision force, we can reach a suitable size of elements in the contact area for predicting behavior more accurately. Figure14 shows the contours of stress in contact direction for different times during the collision; the middle of compression period Figure 14a, the maximum deformation Figure14b, and middle of separation period Figure14c, the last point of contact Figure 14d. We can see that the shape of contour for the middle of the compression period Figure 14a and the middle of the separation period Figure14c is the same. Moreover, the maximum affected area occurs during maximum deformation Figure14b.

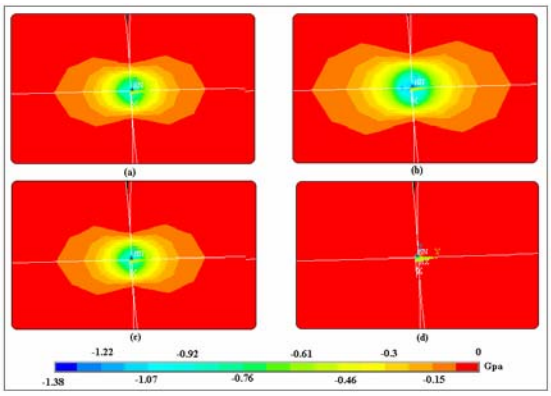

FIG. 14: Contours of stress in contact direction σ_{yy} for a multisize elastic collision in the contact area for the four different steps of the collision. The particles size is $D_1 = 22.2mm$, , $D_2 = 15.9mm$ **,** their properties are listed in Table1 and velocity of impact is equal to 0.5 m/s. (a) The stress contours in middle of the compression period (b) The stress contours in maximum deformation (c) The stress contours in the middle of the separation period (d) The stress contours at the end of the collision.

To demonstrate the usefulness of the finite elements method in the simulation of viscoelastic behavior of collision between two spherical particles of different size, we ran a case using the same mesh with the following material properties. The value of G_0 is found from the following equation: $G_0 = E/2(1+\upsilon) = 2.53\times10^{10} kg/ms$ .The value of the long-time shear modulus G_∞ is set to zero. By using the above-mentioned properties and decay coefficient equal to $\beta = 2.708\times10^3 1/s$, we ran some cases with particles the sizes of $D_1 = 22.2mm, D_2 = 15.9mm$. The result of these simulations conformed well to the experimental results that we explained in section 2.

For example, from the result of this simulation we reached a coefficient of restitution equal to 0.92 for the case of impact velocity equal to $0.5\, m/s$. For the size of the particles and velocity that are mentioned above, we measured the coefficient of restitution equal to 0.925 from the experiment. By comparing these two results, the capability of this method for modeling the viscoelastic behavior of a multisize collision between two glass particles has been shown.

5. Conclusion and Remarks

By using a modified Newton cradle device, some useful experiments have been carried out to measure normal coefficient of restitution in the collision of viscoelastic, multisize glass spherical particles. Analysis of these experimental results leads us to making better understanding of binary collision process between multisize viscoelastic balls. The effect of impact velocity and size of particles on the lost of energy during the collision has been defined by using these experimental results. In a constant impact velocity, we observed that increasing the difference between the sizes of particles would cause decreasing in the coefficient of restitution and vice versa. In monosize collision, the normal coefficient of restitution will decrease with increasing impact velocity but in a constant and certain impact velocity, the amount of this coefficient will increase with increasing the size of balls. By using the aforementioned experimental results, a modified contact force model has been presented for modelling binary collision between the monosize glass balls.

For finding a suitable contact force model for collision of ice balls, we used the experimental data that has been reported by Bridge et al [1] as the reference data. By using this experimental result, we have introduced a new contact force model for collision between ice balls. Indeed, this new model is more accurate than the model presented by Brillantov et al. [2].The new simplified contact force models which have been presented in this article can be used for modeling discrete system and molecular dynamics simulations. For analysing our experimental result for multisize collision between the glass balls, a numerical model based on finite element methods has been developed. Validity of this finite element model has been confirmed by comparing its result for coefficient of restitution with our experimental measured values. The stress behaviour of glass balls during the collision has been addressed by using this accurate finite element model.

References

[1] F.G. Bridges , A. Hatzes and D.N.C. Lin, Structure, stability and evolution of Saturn's rings, *Nature* **309** 333-335 (1984).

[2] N.V. Brilliantov, F. Spahn, J.-M. Hertzsch, and T. Pöschel, *Phys. Rev. E* **53** 5382- 5392 (1996).

[3] P. Cundall and O. A. Strack, A discrete numerical model for granular assemblies, *Geotechnique* **29** 47-65 (1979) .

[4] M. Babic , H.H. Shen and H.T. Shen, The stress tensor in granular shear flows of uniform, deformable disks at high solids concentrations, *Journal of Fluid Mechanics* **219** 81-118 (1990) .

[5] C.S. Campbell, Granular shear flows at the elastic limit, *Journal of Fluid Mechanics* **465** 261-291(2002).

[6] D.Z. Zhang and W J. Whiten, The calculation of contact forces between particles using spring and damping models, *Power Technology* **88** 59-64 (1996).

[7] B. K. Mishra and C. V. R. Murty, On the determination of contact parameters for realistic DEM simulations of ball mills, *Powder Technology* **115** 290-297(2001).

[8] H. Hertz, Uber die Berührung fester elastischer Körper, *J.reine und angewandte Mathematik* **92** 156-171(1882).

[9] T. D. Mindlin, Compliance of elastic bodies in contact, *ASME Journal of Applied Mechanics* **16** 259-268(1949).

[10] O. R.Walton, R. L.Braun, Viscosity, granular-temperature, and stress calculations for shearing assemblies of inelastic, frictional disks , *Journal of Rheology* **30** 949-980(1986).

[11] C.Thornton, Z. Ning, A theoretical model for the stick/bounce behaviour of adhesive, elastic-plastic spheres, *Power Technology* **99** 154-162(1998).

[12] P. Zamankhan, M.H.Bordbar, Complex Flow Dynamics in Dense Granular Flows-Part I: Experimentation**,** *Journal of Applied Mechanics* **73** 648-657(2006).

[13] L. Vu-Quoc, X.Zhang and L. Lesburg, Normal and tangential force-displacement relations for frictional elasto-plastic contact of spheres, *International Journal of Solids and Structures* **38** 6455-6490(2001).

[14] U. Sellgren, S. Björklund and S. Andersson, A finite element-based model of normal contact between rough surfaces, *Wear* **254** 1180-1188(2003).

[15] D. Gugan, Inelastic collision and the Hertz theory of impact, *American J. of Phys.***68** 920-924(2000).

[16] D. B. Marghitu, Y. Hurmuzlu , Three Dimensional Rigid Body Collisions with Multiple Contact Points, *ASME Journal of Applied Mechanics* **62** 725-732(1995).

[17] E. Falcon, C. Laroche, S. Fauve and C. Coste, Behavior of one inelastic ball bouncing repeatedly off the ground ,*The European Physical Journal B* **3** 45-57(1998).

[18] Y.Tsuji, T. Tanaka and T.Ishida, Lagrangian numerical simulation of plug flow of cohesionless particles in a horizontal pipe**,** *Power Technology* **71** 239-250(1992).

[19] W. N. Findley, J.S.Lai, and K.Onaran, *Creep and Relaxation of Nonlinear Viscoelastic Materials (with an Introduction to Linear Viscoelasticity)*, Dover Publications Inc., New York, 1989.

[20] G.Kuwabara, K. Kono, Restitution coefficient in a collision between two spheres, *Japanese Journal of Applied Physics* **26** 1230-1233(1987).

[21] N. V.Brilliantov and T. Poschel, *The Physics of Granular Media, chapter 8: Collision of Adhesive Viscoelastic Particles*, John-Wiley Publications, New York, 2004.

[22] W.A.M. Morgado and I.Oppenheim, Energy dissipation for quasielastic granular particle collisions, *Phys. Rev. E* **55** 1940-1945(1997).

[23] K.H.Hunt, and F.R.E. Crossley, Coefficient of restitution interpreted as damping in vibroimpact, *J. Appl. Mech.* **97** 440-445(1975).

[24] T. Schwager and T. Pöschel, Coefficient of normal restitution of viscous particles and cooling rate of granular gases, *Phys. Rev. E* **57** 650-654(1998).

[25] K-H.Hellwege and O.Madelung, *Physical Properties of Rocks, New Series, Group V, Vol. 1, Pt. a*, Springer, Berlin, 1982.

[26] K.L.Johnson, *Contact Mechanics, 2nd ed.*, Cambridge University Press, New York, 1985.